Multidisciplinary Design and Architecture Optimization of a Reusable Lunar Lander

Laurent Beauregard, Annafederica Urbano, Stéphanie Lizy-Destrez, Joseph Morlier

Multidisciplinary design and architecture optimization of a reusable lunar lander

Laurent Beauregard *, Annafederica Urbano†, Stéphanie Lizy-Destrez‡
ISAE-SUPAERO, Université de Toulouse, France

Joseph Morlier§
ICA, Université de Toulouse, ISAE-SUPAERO, MINES ALBI, UPS, INSA, CNRS, Toulouse, France

With renewed interest in lunar exploration and the upcoming deployment of the lunar space station, the Lunar Orbital Platform-Gateway (LOP-G), the scientific community is focusing on the design of a lander to bring people back to the lunar surface. This work focuses on optimizing two aspects of the lunar lander concurrently: the mission architecture and the vehicle design, often treated independently in the literature. A methodology is introduced to enumerate and preliminarily rank all possible mission architectures. The best mission architectures are then coupled with a multidisciplinary design optimization process by modeling the various components of the spacecraft and optimizing over a set of design parameters. The need for fast computational models, particularly in trajectory optimization, resulted in an analytical approximation of gravitational losses. This work resulted in a hierarchy of mission architectures that are ranked according to the average mass necessary to perform the mission. This work is intended to help a system engineer designing a lunar lander in choosing the best number of vehicles, the number of reuses and the mission profile for his/her mission requirements.

Nomenclature

BOR	=	Boil-off rate
CEA	=	Chemical Equilibrium with Application
$CR3BP$	=	Circular Restricted Three Body Problem
GNC	=	Guidance, Navigation and Control
$IPOPT$	=	Interior Point Optimizer
$LH2$	=	Liquid Hydrogen
$LCH4$	=	Liquid Methane

*PhD candidate
†Researcher
‡Associate Professor
§Professor

LOX	=	Liquid Oxygen
LLO	=	Low Lunar Orbit
$LOP-G$	=	Lunar Orbital Platform-Gateway
MER	=	Mass Estimating Relationship
MDO	=	Multidisciplinary Design Optimization
$NASA$	=	National Aeronautics and Space Administration
$NRHO$	=	Near Rectilinear Halo Orbit
NTO	=	Nitrogen Tetroxide
$RP-1$	=	Rocket Propellant-1
$SLSQP$	=	Sequential Least SQuares Programming
SLS	=	Space Launch System
$SNOPT$	=	Sparse Nonlinear Optimizer
Isp	=	Specific impulse [s]
SMT	=	Surrogate Modelling Toolbox
TWR	=	Thrust to Weight Ratio
$UDMH$	=	Unsymmetrical Dimethylhydrazine
ZBO	=	Zero boil-off

I. Introduction

50 years ago humanity stepped for the first time on the lunar surface. Nowadays a new space race is underway to bring people back onto the lunar surface. The international community has agreed to deploy an orbital station around the Moon, named the Lunar Orbital Platform-Gateway (LOP-G) in the 2025 timeframe. This station is planned to be used as a hub. The crew would first travel to the LOP-G, there they would transfer to a lander to reach the lunar surface. Their return would pass by the LOP-G to transfer back into the Orion capsule, allowing a return to Earth. While it has been decided that the Space Launch System (SLS) and Orion will bring people to and from the LOP-G, the vehicle that will bring the crew unto the lunar surface has not been finalized yet. Several architectures have been proposed in the past, including by Lockheed Martin [1] which proposed a reusable one stage lander with liquid hydrogen as fuel. Another proposal was by NASA with the Altair [2] lander: a two-stage lander similar to Apollo with the landing stage using hydrogen and the upper stage using storable propellants. Due to the high cost of bringing materials and people around the Moon, it is vital that the vehicles are optimized with a metric that correlates strongly with the total cost of the mission. To obtain an optimal vehicle architecture according to this metric, Multidisciplinary Design Optimization (MDO) will be employed. MDO techniques have gained significant traction in

the last decades and been applied in the field of aerospace engineering, including airplane design [3] with aeropropulsive design optimization, expendable launcher design [4] with global and local optimization approach, reusable launchers design [5] with multilevel, multimission, decoupled MDO formulation and satellite design [6] with millions of design variables. In this work a MDO tool developed by NASA Glenn Research Center called OpenMDAO will be used. OpenMDAO has seen several successful applications [7]. A vast amount of work has been done on lunar landers/orbiters, analyzing in detail their components such as the propulsion system, structure, life support system, reusability, maintenance, GNC and so on [8][9][1]. Recent work has focused on a MDO approach to reusable lunar cargo lander design [10].

In the context of this article, a mission architecture is defined as: Number of vehicles, sequence of transfers and number of reuses. The choice of these variables impacts massively the lunar lander design process. Work on simultaneous trajectory and vehicle optimization for a lunar supply chain have been done before [11]. However, for lunar lander missions, there is a lack of literature that treats the optimization of the mission architecture and the vehicle design concurrently. Most literature on lunar landers consider either fixed mission architecture, or only a few alternative choices [8]. The present work aims at pushing an understudied aspect of the lunar mission design: the concurrent optimization of the mission architecture and vehicle design. This is done in a two-step optimization process. In the first step, a systematic approach to generate all possible mission architectures is introduced. Those mission architectures are then classified using a basic metric. This first step in known in the literature as the exhaustive enumeration (EE) method or combinatorial optimization [12]. For the second step, the best mission architectures are combined with a multidisciplinary design optimization process to obtain a series of optimal vehicle designs. The workflow for this article is shown in Fig. 1. The result of this study is a ranking of the mission profiles and the number of reuses as a function of the average mass to perform the mission. The relevant results will be compared to NASA's proposed "Notional Human Landing System Reference Architecture" [13]. The complete results are displayed in tables 10, 11 and 12. The goal of this work is to assist a system engineer in choosing the best mission architecture for a lunar mission.

This paper is composed of 7 chapters. The underlying theory and methods used throughout this work will be introduced in section II. Section III explores the first phase of the work: mission architecture enumeration. Section IV presents the engineering models for each subsystem considered for the lunar lander. The list of tools used in this article is shown in figure 1. Section V will consider the MDO process, the objective function and the optimization. Section VI will present the results obtained and, lastly, section VII will conclude this work. As seen in figure 1, this research is broken down into two parts. First, the mission architectures are exhaustively enumerated in a discrete way. A MDO framework is then built to analyze the vehicles. Finally the MDO framework is coupled with the mission architectures to produce a family of preliminary designs of optimized vehicles.

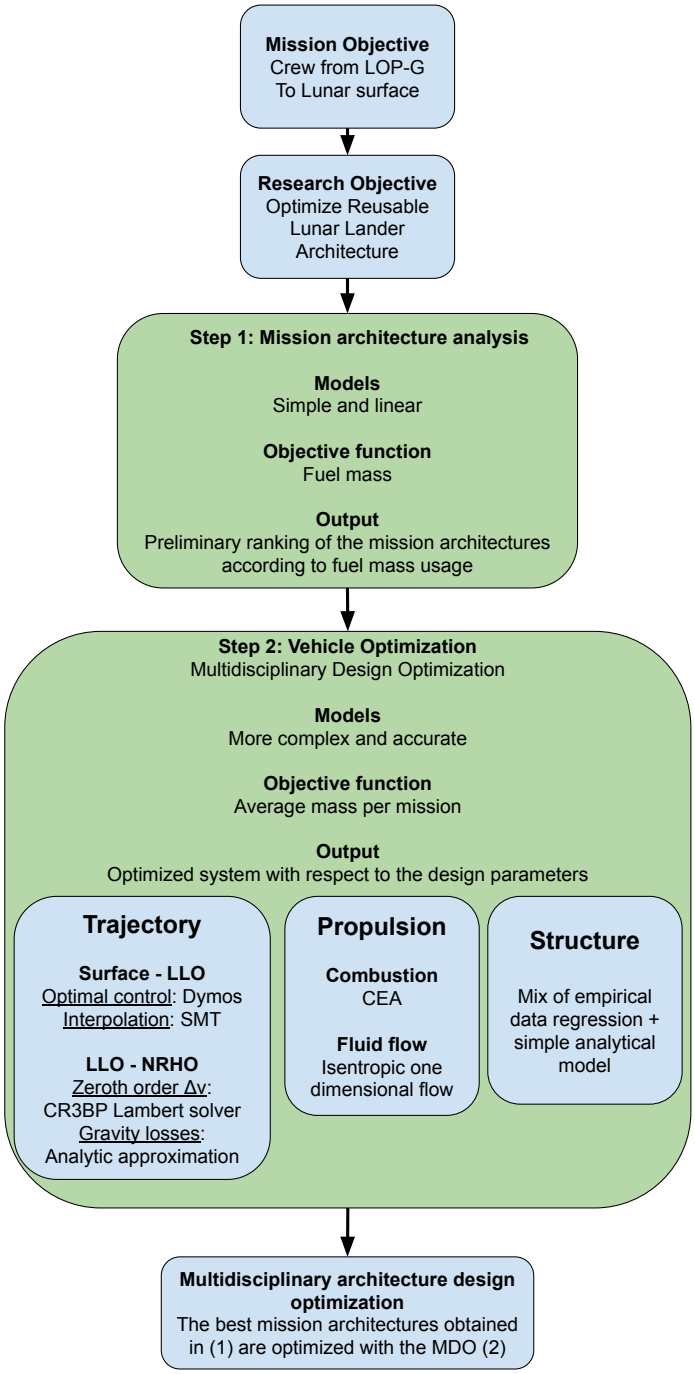

Fig. 1 Schematic of the workflow and tools used in this work.

II. Theory and methods

To describe and optimize the lunar lander, several tools are used. First, the field of multidisciplinary design optimization (MDO) is described in II.A. Optimal control theory is introduced in II.B. Lastly, section II.C deals with the models of orbital mechanics used in this work. The tools of mission architecture enumeration and engineering models of the lunar lander subsystems will be described in their own sections in III and IV respectively.

A. Multidisciplinary design optimization

A multidisciplinary design optimization problem can be brought into the following canonical form: [14]:

$$\min_{x,y,z} F(x, y, z) \tag{1a}$$

Subject to

$$y = C(x, y, z) \tag{1b}$$

$$0 = R(x, y, z) \tag{1c}$$

$$0 \leq g(x, y, z) \tag{1d}$$

where $x \in \mathbb{R}^N$ are the design variables, $y \in \mathbb{R}^D$ are the coupling variables and $z \in \mathbb{R}^S$ are the state variables.
N is the number of design variables of the system, D is the number of coupling variables of the system, S is the number of state variables necessary to describe the system. I is the number of inequality constraints.
$F : U_F \subseteq \mathbb{R}^N \times \mathbb{R}^D \times \mathbb{R}^S \to \mathbb{R}$ is the objective function to be minimized.
$C : U_C \subseteq \mathbb{R}^N \times \mathbb{R}^D \times \mathbb{R}^S \to \mathbb{R}^D$ represents the disciplines of the system.
$R : U_R \subseteq \mathbb{R}^N \times \mathbb{R}^D \times \mathbb{R}^S \to \mathbb{R}^S$ are the residual of the state variables describing the system.
$g : U_I \subseteq \mathbb{R}^N \times \mathbb{R}^D \times \mathbb{R}^S \to \mathbb{R}^I$ represents the inequality constraints of the system.
To numerically solve these optimization problems, a nonlinear program software must be used. Examples of commonly used software include IPOPT[15], SNOPT[16] or SLSQP[17]. In this work, the MDO framework used is NASA's python library OpenMDAO [7].

B. Optimal control

Several instances of optimization problem must performed over a set of functions. A special case of those are called optimal control problems. Most optimal control problem can be brought into the form [18]:

$$\min_{u} \{S\} \tag{2a}$$

Where

$$S = \int_{t_0}^{t_f} \mathcal{L}(t, x, u)\, dt + \phi(t_0, x_0, t_f, x_f) \tag{2b}$$

Subject to

$$\dot{x} = f(t, x, u) \tag{2c}$$

$$0 = \Psi(t_0, x_0, t_f, x_f) \tag{2d}$$

Where t_0 is the initial time, t_f is the final time, x_0 is the initial state and x_f is the final state, S is the (scalar) cost function to be minimized over the trajectory, $u(t)$ is the control of the system which must be found, $x(t)$ is the state of the system, f is the dynamics of the system, $\mathcal{L}$ is the running cost, ϕ is the boundary cost and Ψ is the boundary constraint.

In this work, the software used to deal with optimal control problems is DYMOS, a python subpackage of OpenMDAO [19]. It is a direct method that uses a Gauss-Lobatto [20] or Radau Pseudospectral [21] direct transcription method to convert the optimal control problem into a non-linear program, for which the optimization software described at the end of section II.A can be used. In this particular work, the Gauss-Lobatto method was used due to lower computational time.

C. Orbital mechanics

Two orbital models are used in this work depending on the location of the orbiter. At lunar launch and in low lunar orbit (LLO), the gravity of the Moon dominates the dynamics and so two-body dynamics is considered. For farther orbits, e.g. near the LOP-G, the dynamic of trajectories are modeled by an Earth-Moon circular restricted three-body problem (CR3BP) [22].

1. Low Lunar Orbits

For the lunar surface to low lunar orbit (LLO) trajectory, the gravity of the Moon dominates. During an ascent and descent it can be assumed that the motion is restricted to a plane [23]. In an inertial frame around the Moon, the dynamics can be described by the following system of equations:

$$\dot{r} = v_r \tag{3a}$$

$$\dot{\theta} = \frac{v_t}{r} \tag{3b}$$

$$\dot{v}_r = -\frac{\mu}{r^2} + \frac{v_t^2}{r} + \frac{T}{m}\sin(\alpha) \tag{3c}$$

$$\dot{v}_t = -\frac{v_r v_t}{r} + \frac{T}{m}\cos(\alpha) \tag{3d}$$

$$\dot{m} = -\frac{T}{g_0 I_{sp}} \tag{3e}$$

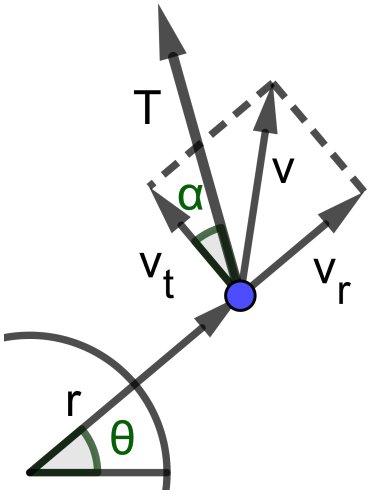

Fig. 2 Geometry of low lunar orbit dynamics

Where r is the radial position of the spacecraft, θ is the angular position of the spacecraft, v_r is the radial component of the velocity, v_t is the tangential component of the velocity, m is the mass of the spacecraft, T is the thrust of the spacecraft, $g_0 = 9.80665\ \mathrm{m/s^2}$ is the standard gravity, I_{sp} is the specific impulse of the rocket engine and α is the angle

of attack of the spacecraft.

2. Circular restricted three body problem

For objects that orbit farther than low lunar orbit, the gravity of the Earth must be accounted for. The model chosen in this work is the CR3BP which assumes that i) only the gravity of the Earth and the Moon are considered and ii) the Moon and the Earth have circular orbits. Usually the dynamic is expressed in the rotating frame of the Earth-Moon system whose origin is the center of mass of the system. In that case, the equation of motions are:

$$\ddot{\vec{r}} = -\frac{\mu_E}{|\vec{r}-\vec{r}_E|^3}(\vec{r}-\vec{r}_E) - \frac{\mu_M}{|\vec{r}-\vec{r}_M|^3}(\vec{r}-\vec{r}_M) - \vec{\omega}\times(\vec{\omega}\times\vec{r}) - 2\vec{\omega}\times\dot{\vec{r}} \tag{4}$$

Where $\vec{r}$ is the vectorial position of the spacecraft, $\vec{r}_E$ and $\vec{r}_M$ are the vectorial positions of the Earth and Moon respectively (at rest in the rotating frame), μ_E and μ_M are the standard gravitational parameters of the Earth and Moon, $\vec{\omega}$ is the angular rotation vector of the Earth-Moon system.

The rich dynamics of this system has been studied extensively and several periodic orbits of the CR3BP exist [24]. A class of well-known orbits is called halo orbits. Earth-Sun and Earth-Moon halo orbits have been successfully used for spaceflight missions such as LISA Pathfinder and Chang'e 4. The LOP-G will be placed on a subcategory of halo orbits called Near Rectilinear Halo Orbit (NRHO).

III. Mission architecture enumeration

A mission architecture is a specific sequence of transfers and maneuvers between different orbits and spacecrafts in order to achieve a particular objective. A large set of mission architectures exist which could be used to bring a crew from the LOP-G to the surface and back. In this chapter, a systematic way of considering all mission architectures is described. While more sophistical optimization techniques could be used, such as branch and bound [25], combinatorial optimization was found to be sufficient for this application. Graphically, the architecture can be represented by graphs similar to Fig. 3. In particular Fig. 3 represents a one stage architecture; the vehicle starts at the NRHO, performs a transfer to LLO, then to the lunar surface, then launch from the surface to reach LLO again and, lastly, returns to the NRHO. This diagram can also be shortened by the one on the right with the label "1" indicating the vehicle 1 is performing the transfers. To ensure an exhaustive search of the mission architectures, a general description of the framework of orbital transfers has to be constructed. The following 3 basic parameters will be used to parametrize the architectures: the number of valid locations, N_S, the number of vehicles, N_V and the number of allowed transfers, N_F. In this work $N_S = 3$, that is, only 3 locations are considered: the orbit of the LOP-G (NRHO), the low lunar orbits (LLO) and the lunar surface. While an arbitrary amount of vehicles and transfers could be considered, the search complexity grows exponentially with those variables:

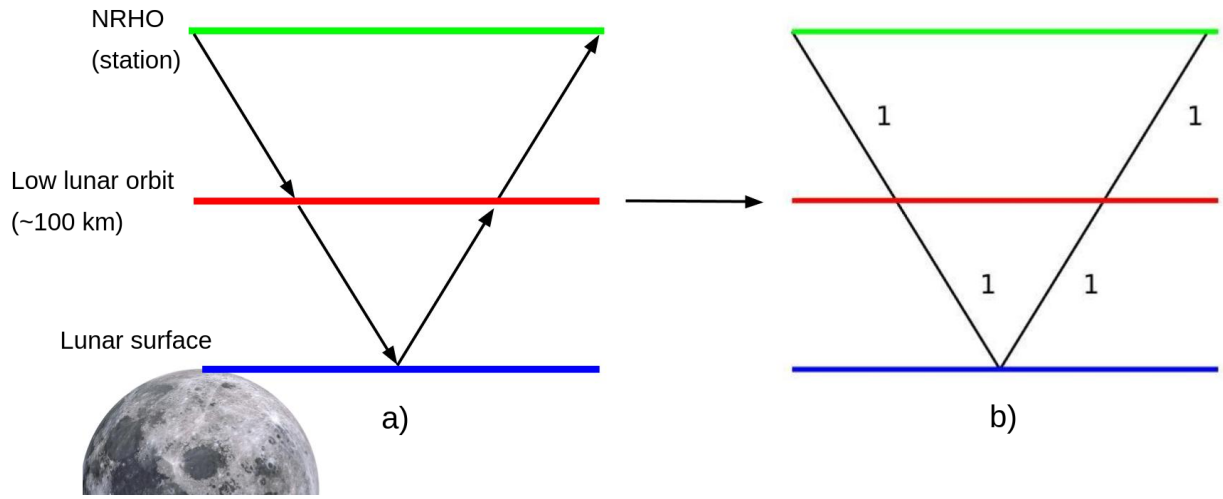

Fig. 3 Schematic of the mission with a single vehicle.

the number of possible architectures to check is bounded above by $N_S^{N_V(N_F+1)}$. This research will focus on the most promising cases; the number of vehicles N_V will be varied from 1 to 3, (3 being the number Apollo used: service module, ascent and descent stages [26]). The number of allowed transfers N_F will be varied from 4, the minimum to achieve the mission, represented in Fig. 3, to 6 transfers. Beyond 6, the search space is too large to compute with the available tools and techniques. Moreover, as orbital transfers are very expensive in terms of fuel, the optimal mission architectures will necessarily have a low number of transfers. Therefore, there is no drawback to searching only for a low number of transfers.

When N vehicles travel on the same trajectory there are exactly:

$$\sum_{n=1}^{N} \binom{N}{n} n^{N-n} \tag{5}$$

number of different ways of arranging the transfers. The first few values are shown in Table 1.

Table 1 Number of rearrangements

Number of vehicles traveling on the same path	# rearrangements
1	1
2	3
3	10
4	41
5	196

The explicit construction of the 10 cases for $N = 3$ is shown in the appendix 14. Because of the sheer number of architectures to consider, a simple and fast mass model to order the architectures had to be considered. The mass model,

at this stage, is given by several linear relations between the variables [27]:

$$M_{Total} = M_P + M_S + M_T + M_F \tag{6a}$$

$$M_F = M_{Total}\left(1 - e^{-\Delta v/(g_0 I_{sp})}\right) \tag{6b}$$

$$M_T = \alpha M_F \tag{6c}$$

$$M_S = \beta M_{Total} \tag{6d}$$

Where M_P is the payload mass of the spacecraft, M_F is the fuel mass of the spacecraft, M_T is the tank mass of the spacecraft, M_S is the structure mass of the spacecraft, M_{Total} is the total mass of the spacecraft, α is the tank to fuel mass ratio, β is the structural efficiency (structure/total mass) and Δv is the velocity increment of the stage. The values of $\alpha = 0.05$ and $\beta = 0.15$ were chosen according to the work of [27].

Due to the simplicity of the system, it is possible to write the solution of these equations in closed form as:

$$M_{Total} = \left(\frac{1}{(1+\alpha)e^{-\Delta v/(g_0 I_{sp})} - \alpha - \beta}\right) M_P \tag{7}$$

Once the mission architectures are generated, a metric must be introduced to order them. At this stage, the metric chosen is not critical since this analysis is only to remove extremely inefficient architectures. Since the vehicles are meant to be reusable, the simple metric used is the amount of fuel per mission. This metric allows one to obtain a preliminary ranking of the various mission architectures. Examples of mission architectures are graphically represented in Fig. 4a to 4d. The number labeling refers to which spacecraft is performing the maneuver. Double and triple lines indicates vehicles moving together, with the first number being the vehicle that provides the thrust. For this analysis, the sole goal is to bring spacecraft "1" to the lunar surface and back at the NRHO. After taking into account combinatorial duplicates, there remain several mission architectures that, while theoretically valid, require strictly more fuel than another mission architecture. Example 4c shows a loop of vehicle "2" from LLO to NRHO, this loop is a strict waste considering the sole purpose of bringing spacecraft "1" on the surface and back. Example 4d has vehicle "3" coming back from the surface to LLO, this maneuver is strictly unnecessary in the context of bringing spacecraft "1" to the surface and back. These architectures could have niche applications but, for the purpose of this study, any architecture which is strictly inferior in terms of mass than another one is discarded. Table 12 and 13 of the appendix show all mission architectures considered in this work. Table 13 and 14 enumerate the characteristics of each of the mission architectures.

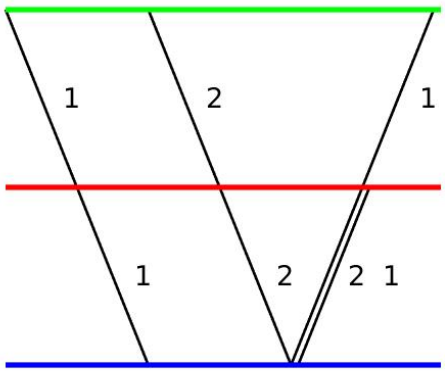

(a) Two vehicles architecture

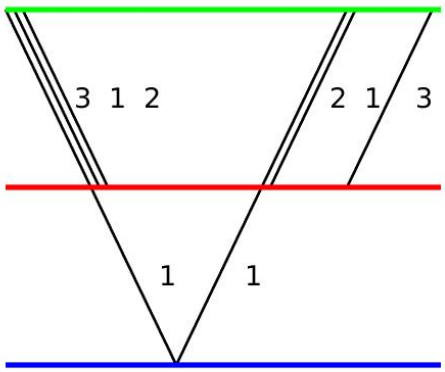

(b) Three vehicles architecture

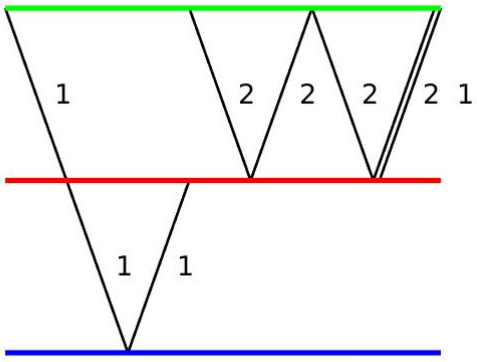

(c) Two vehicles architecture with vehicle "2" performing a loop (discarded)

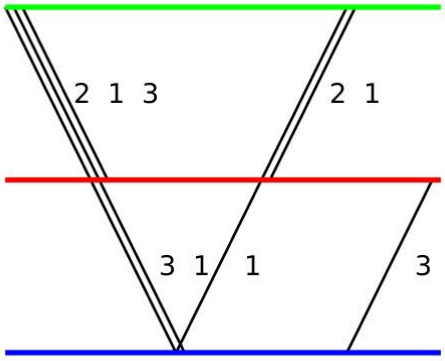

(d) Three vehicles architecture with strictly inferior properties because the last transfer of vehicle "3" serves no purpose (discarded)

Fig. 4 Mission architecture examples

IV. MDO model description

In this section, the physical models of the spacecraft will be introduced. Discipline models are needed to build the MDO tool. In particular, three disciplines are considered: propulsion, trajectory and structure as shown in an extended design structure matrix in Fig. 5. The MDO process also needs an objective function to optimize the vehicles; this will be introduced in the next section.

A. Propulsion

Since the vehicle is intended to carry humans and be refuelable in orbit, only liquid-fueled propulsion systems will be considered in this work. For these types of applications, 4 different types of propellant are usually considered [29]

- LH2/LOX: Liquid hydrogen + Liquid Oxygen
- LCH4/LOX: Methane + Liquid Oxygen
- RP-1/LOX: Rocket propellant-1 + Liquid Oxygen

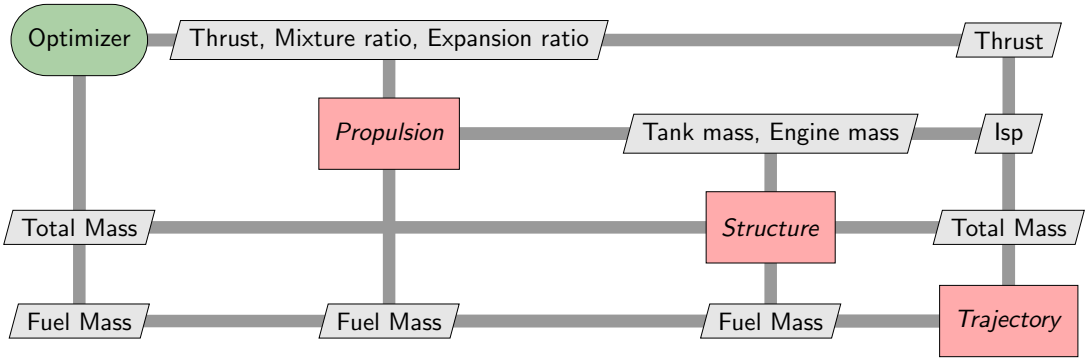

Fig. 5 Extended design structure matrix for the lunar lander with the three disciplines of trajectory, propulsion and structure.

Table 2 Inputs/Outputs for propulsion module [28]

Inputs	Dimension	Outputs	Dimension
Type of fuel	-	Specific impulse, I_{sp}	s
Mixture ratio	-	Combustion temperature	K
Combustion pressure	Pa	Molecular weight	g/mol
Expansion ratio	-	Adiabatic index	-
Maximum thrust	N	Engine mass	t

- UDMH/NTO: Hydrazine based compounds + Nitrogen tetroxide

The propulsion module is modeled in three steps, first, the combustion analysis is performed using Chemical Equilibrium with Applications (CEA), the NASA developed state of the art combustion analysis software [30]. Then the fluid flow is modeled by an isentropic one-dimensional flow through a convergent-divergent nozzle [31]. Lastly the mass of the engine is obtained via a multitude of Mass Estimating Relations (MER) [32]. While the software has been developed for all 4 propellants above, only the results for LH2/LOX will be shown. This allows a more direct comparison with the recent LH2/LOX Lockheed Martin lander. Figures 6 shows the Isp results of the propulsion module for a combustion pressure of 30 bar. The optimality line of best mixture ratio for a given expansion ratio is also shown.

B. Structural, thermal and mass analysis

Table 3 Inputs/Outputs for structural and thermal module

Inputs	Dimension	Outputs	Dimension
Density of fuel	kg/m^3	Fuel tank mass	t
Density of oxidizer	kg/m^3	Oxidizer tank mass	t
Mixture ratio	-	Cooling system mass	t
Tank material	See Table 5	Structural mass	t
Total propellant mass	t		

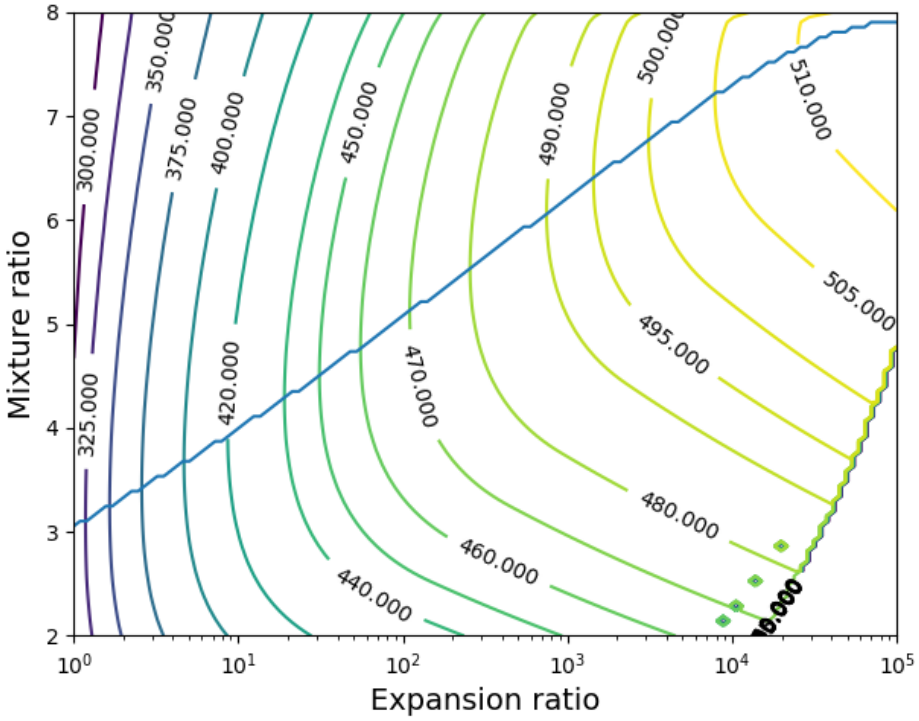

Fig. 6 LH2/LOX specific impulse (s) as a function of mixture and expansion ratio. Calculated using CEA [30].

Two vehicle types are considered in this work: a crew vehicle that can host 2-4 astronauts for a duration of 1 month and transportation systems. Each one of these vehicle has an associated inert mass as shown in Table 4. According to

Table 4 Fixed mass for the two types of vehicles

	Payload mass	Comments
Crewed module mass (t)	12	Based on the Orion spacecraft [33]
Transportation vehicle invariant mass (t)	0.4	Based on [8]

Humble [32], the tank mass can be based on a simple hoop analysis of thin pressure vessels with corrective factors. Those assumptions allow the mass of the tank M_t to be proportional to the mass of fuel (or oxidizer) inside the tank M_F:

$$M_t = N_{real}\left(2\frac{\rho_t}{\rho_F}\frac{P}{\sigma}\right)M_F \tag{8}$$

with ρ_t the density of tank material, ρ_F the density of the fuel (or oxidizer), the operating pressure of the tank P and the allowable stress of the material σ. The allowable stress of the pressure vessel is usually half (safety factor of 2) of the ultimate strength of the material $\sigma = \frac{1}{2}\sigma_{max}$. The actual mass of the tank is typically 2 to 2.5 times larger than the theoretical value, this is encoded in N_{real}. To be conservative, the value of $N_{real} = 2.5$ was chosen in this work. The

choice of tank material is in itself a large subject. For simplicity, aluminum 2219 was chosen because of its history in the space sector[32]. Its relevant properties can be found in Table 5.

Table 5 Physical properties of aluminum 2219

Density (kg/m^3)	Ultimate strength (GPa)
2800	0.413

As for the mass of the structure, landers and orbiters have different stress requirements [32] [9]. Order of magnitude estimate of the structural mass for orbiters and landers are: 15% of the dry weight for orbiters and 35% of the dry weight for landers.

For vehicles involving cryogenic propellant, like hydrogen, oxygen and methane, heat management is primordial to prevent excessive boiloff. Thermal control essentially falls into two categories, passive and active cooling. In passive cooling, the tanks are heavily insulated and the liquids are routinely vented to prevent pressure build-up inside the vessel. While the boil-off rate (BOR) depends on the nature of the system, the quality of its insulation, geometry and exposure to the sun etc, some order of magnitude are available in the literature [34], hydrogen BOR: 0.127% /day = 3.81% /month, oxygen BOR: 0.016% /day = 0.48% /month and methane BOR: 0.016% /day = 0.48% /month. When passive cooling is not sufficient for the mission, active cooling may be employed to keep the fuel and oxidizer from boiling away. The situation where all boil-off is prevented is called the zero boiloff (ZBO) condition. To achieve this state, a cryocooler must be used to remove heat leaks into the tank. At temperatures of liquid hydrogen, the efficiency of a cryocooler is in the order of 0.1%, requiring 1 kW of electricity to remove 1 W of heat. Oxygen and methane however are stored at a much higher temperature and so cryocoolers in that range have a 2% efficiency [35]. For a cylindrical vessel of constant radius, the heat leak scales proportionally to the mass of the fuel. Since the mass of the power system scales approximately linearly to the power required, this ultimately implies an approximately linear relationship between the mass of the cooling system and the mass of the propellant. The following relation is obtained:

$$M_{cooling} = \left(\frac{2kI}{r\rho_F\epsilon}\right) M_{fuel} = \alpha_{\text{cooling}} M_{fuel} \tag{9}$$

where k = 25 kg/kW is the amount of mass necessary to generate a given power with solar arrays [36], I = 0.4 W/m^2 is the heat leakage rate of an insulated tank [37], r $\sim$ 1 m is the radius of the cylindrical tank, ρ_F is the density of the fuel and ϵ is the efficiency of the cryocooler. The proportionality constant can be estimated, $\alpha_{\text{cooling}} = 0.3$ for hydrogen and $\alpha_{\text{cooling}} = 0.01$ for methane/oxygen. In this work, only active cooling was considered. Further detailed comparison of thermal management systems should reconsider passive cooling as well.

C. Trajectory analysis

Table 6 Inputs/Outputs for trajectory module

Inputs	Dimension	Outputs	Dimension
Thrust	N	Propellant mass	t
Total vehicle mass	t	Maneuver Δv	m/s
Specific impulse, I_{sp}	s	-	-

One of the fundamental disciplines of any spacecraft is the analysis of its trajectory. In this work, the spacecraft must be able to operate between a NRHO, a low lunar orbit (LLO) and the surface of the Moon. Approximate values for the Δv requirements are given in Table 7 [38]. To consider the gravity losses due to design variation in the TWR and Isp, the trajectory analysis must be part of the optimization process.

Table 7 Approximate Δv requirement

Transfer	Δv (m/s)
NRHO <–> LLO	750
LLO –> Lunar surface	2100
Lunar surface –> LLO	1900

1. NRHO to LLO

The first phase of the transfer will move the spacecraft from the NRHO to the LLO. As a zeroth-order approximation, the transfer Δv was obtained in this work via optimization of the Lambert problem [39]. For the CR3BP, this value is approximately 750 m/s and agrees well with the literature [38]. However, the exact Δv requirement for a particular mission depends on various components of the spacecraft, the most important factors being the thrust to weight ratio and the specific impulse. The gravity losses (or gravity drag) of a maneuver is the difference between the actually Δv spent and the idealized Δv_{inst} with an instantaneous burn.

As a novel contribution, an analytical expansion of the gravity losses as a function of the maneuver time t_f was found. The spacecraft starts on a circular orbit and applies a prograde burn with the objective to change the apoapsis or periapsis. This expansion is done in MATLAB symbolic toolbox and is truncated to order t_f^4:

$$\Delta v - \Delta v_{\text{inst}} \sim \frac{1}{48}\frac{\mu}{r^3}A_0 t_f^3 - \frac{1}{32}\sqrt{\frac{\mu}{r^5}}A_0^2 t_f^4 + \frac{1}{96}\frac{\mu}{r^3}\frac{A_0^2 t_f^4}{g_0 I_{sp}} \tag{10}$$

where Δv is the actual cost to perform the maneuver, Δv_{inst} is the idealized cost assuming instantaneous maneuvers, A_0 is the initial acceleration of craft and r is the distance from the body at which the maneuver is performed. This formula

is similar to Robbin's gravity loss formula [40]:

$$\Delta v - \Delta v_{\text{inst}} \sim \frac{1}{24}\frac{\mu}{r^3}A_0 t_f^3 \tag{11}$$

Equation 10 used in this article contains higher order terms than Robbin's formula, hence it is more precise. Moreover, the boundary conditions assumed in deriving Robbin's formula are that the starting and ending orbits are fixed. Those conditions are stricter than the ones in this article. Thus, in this case, Robbin's formula overestimates the losses by a factor of 2.

2. LLO to Surface

The second phase of the transfer involves landing or taking off from the lunar surface. Considering first the takeoff, it is clear that the initial thrust must overcome the weight $F > m\frac{\mu}{r^2}$. There are several ways to report the "cost to orbit" of a particular spacecraft, two of which are the fuel fraction ζ and the Δv:

$$\zeta = \frac{M_i - M_f}{M_i} = \frac{F}{m_0}\frac{t_f}{g_0 I_{SP}} \tag{12}$$

$$\Delta v = g_0 I_{SP} \ln\left(\frac{m_0}{m_0 - \frac{F}{g_0 I_{SP}} t_f}\right) \tag{13}$$

When ascending from the lunar surface, the ground must be cleared fast enough to prevent collision with the ground. In this work, the following simple geometric constraint was employed:

$$r(\theta) \geq R + \frac{\theta}{\frac{\theta}{h_{\text{min}}} + \frac{1}{kR}} \tag{14}$$

where R is the radius of the moon, h_{min} is the altitude clearance and k is the initial slope of the constraint. Those constraints are shown geometrically in Fig. 7.

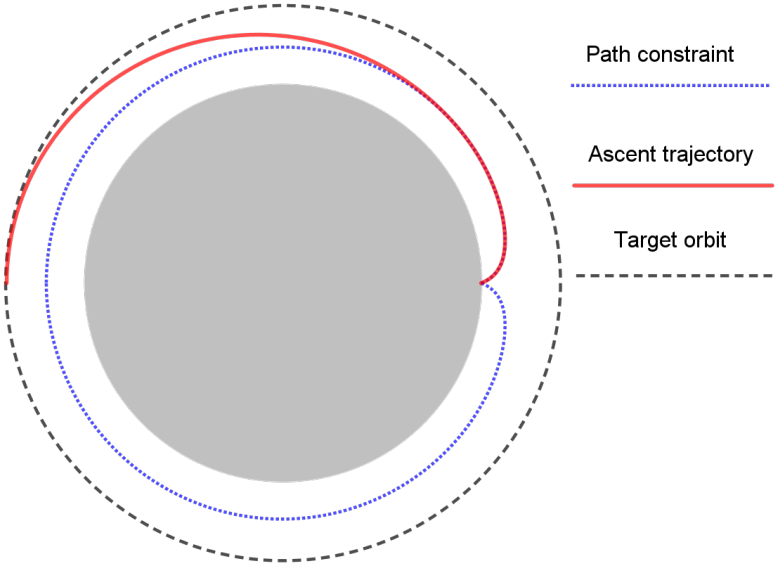

Fig. 7 Geometry of the ascent trajectory (Not to scale)

The optimal control of the trajectory described by equations 3a to 3e with the control variable α is solved using DYMOS with a Gauss-Lobatto transcription of order 3. Fixing the parameters $k = 10$ and $h_{\min} = 6$ km, the resulting fuel fraction can be calculated. A sample plot of the state and control variables is shown in 8. The solutions are calculated for a 20x20 uniform grid with $1 < TWR < 4$ and 250 s$< I_{sp} <$ 500 s and is shown in Fig. 9. To interpolate the grid, the Python library Surrogate Modelling Toolbox (SMT) is used [41].

V. MDO optimization specification

A. Objective function

Several optimization metrics for aerospace vehicles have been used throughout the literature, including maximization of the payload at fixed total mass [28], minimization of cost [42], minimization of the dry weight [28] and minimization of the total mass [28]. While cost models are sometimes used as the metric, it is common, in the preliminary phase of the design, to use the mass of the vehicle as the objective function as a substitute for cost assessment. In this work, the objective function to minimize is the average mass M_{av} necessary to accomplish the mission. The choice of this objective function assumes that one of the most important parameter to minimize for all lunar missions is the mass that must be sent to cis-lunar space, regardless of the nature of the mass itself. The objective function is thus given by:

$$F_{\text{Objective}} = M_{\text{av}} = \frac{M_{\text{total}} + N_{\text{reuse}} \left(M_{\text{expendable}}\right)}{1 + N_{\text{reuse}}} \tag{15}$$

Where N_{reuse} is the number of times the system can be reused, M_{total} is the total mass of the system and $M_{\text{expendable}}$ is the mass necessary to refurbish the vehicles every mission, such as the fuel mass or expendable stages.

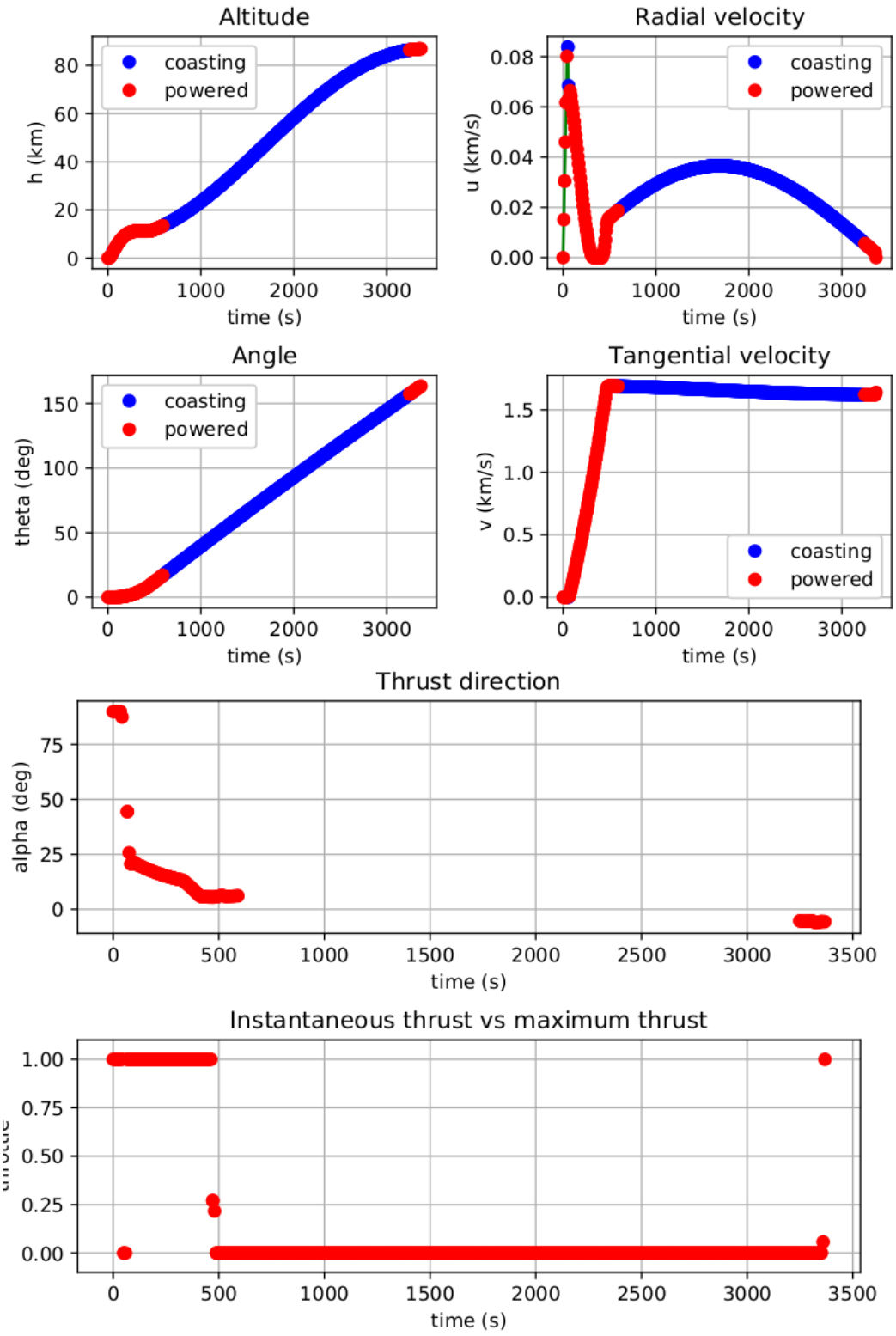

Fig. 8 Sample optimal control for an ascent trajectory with path constraints. Initial TWR = 1.95, Isp = 309 s. Calculated using Dymos [19].

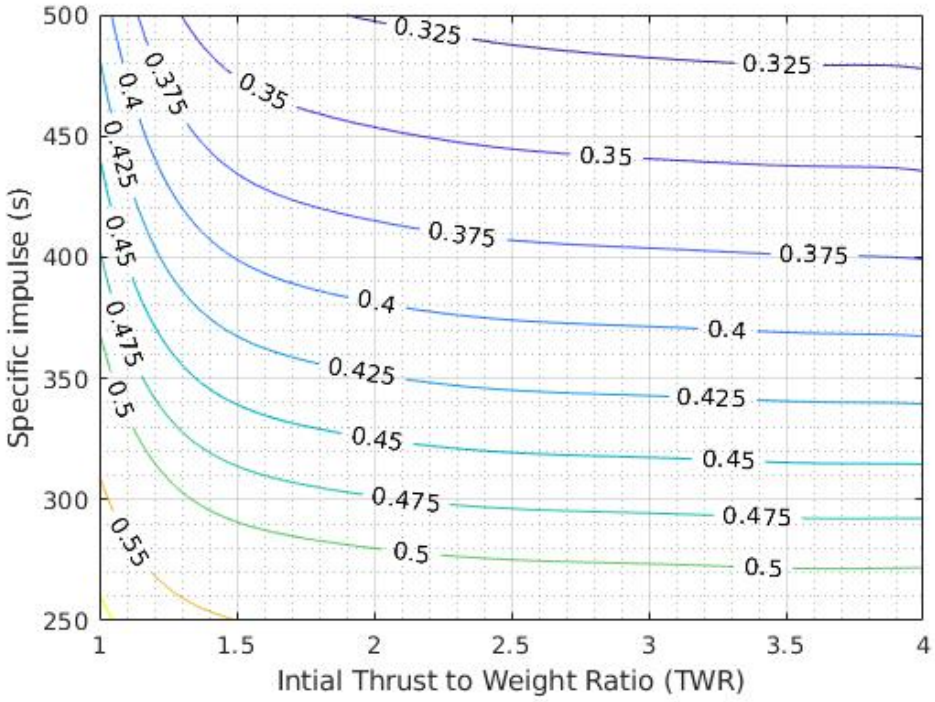

Fig. 9 Fuel mass fraction ζ for lunar take-off as a function of Isp and TWR. Calculated using Dymos [19], interpolated using SMT [41].

B. Optimization

For the optimization of the lunar vehicles, the following assumptions are made: all vehicles use hydrogen and oxygen as propellants and the number of reuses vary from 0 to 6. Each vehicle has its own thrust, expansion ratio and mixture ratio, which will be optimized, for a total of 3 optimization variables per vehicle. For 2 and 3 vehicles, all 20 mission scenarios are considered. The bounds on the design variables are shown in Table 8. In this model there is only

Table 8 Bounds on the design variables

Variable	Min	Max
Thrust (kN)	10	400
Expansion ratio	10	1000
Mixture ratio	2	8

one constraint: for vehicles that land on the lunar surface, the thrust has to be greater than the weight at touchdown and takeoff:

$$\text{Thrust} \geq \text{Weight}_{\text{Touchdown/Takeoff}} \tag{16}$$

This constraint can be said to be "unrelaxable" [43], that is, the output of the model does not exist if this constraint is not respected. In this particular case, the Δv would be infinite or undefined. On a Intel® Core™ i7-4800MQ CPU

@ 2.70GHz × 8, it takes on average 8 seconds to optimize a one stage lander, 35 seconds for a two stage lander and 70 seconds for a three stage lander. It takes on average 2 hours to optimize all 41 mission architecture with 7 reuses ($7 \times 8\ s + 7 \times 20 \times 35\ s + 7 \times 20 \times 70\ s \sim 2$ hours). To avoid local minima, the standard technique of multi-start is employed with 30 initial states randomly chosen in the design space. The total runtime was thus about 60 hours. The local optimization is performed by a SLSQP algorithm with a relative tolerance of 1e-6 as a termination criterion and maximum number of iterations of 100. If an initial guess does not satisfy the unrelaxable constraint 16, the optimization is started over with a newly randomized initial point.

VI. Results and discussion

The best performance obtained is for a 2 vehicle architecture with 6 reuses, with an average mass of 46.0 t. In contrast, a one-stage expendable lander has a total mass of 80.2 t, an increase of 74% compared to the best one. The mass breakdown for selected mission architecture is shown in Table 9. The results of a one-stage lander can be found in Appendix Table 10 for a number of reuses from 0 to 6. For 2 and 3 vehicles and for the number of reuse varying from 0 to 6, the vehicles were optimized for each of the 20 mission architectures. Table 11 and 12 in the appendix shows all the possible cases with the ordering of the best 20 mission architectures with the percentages increase in average mass as compared to the best mission architecture (46 t). As a point of comparison, the Lockheed Martin Lunar Lander would be reused from 4 to 10 times [1] and has a wet mass of 62 t and a dry mass of 22 t. This can be compared to the results obtained in this article for a one-stage 6 times reusable lunar lander with a wet mass of 80.3 t and a dry mass of 25.3 t. More generally, for one stage landers with multiple reuses, the average mass per mission is shown in Fig. 10a. As the number of reuse increases, the average mass necessary to complete the mission decreases. It is important to note the diminishing return behavior as the number of reuse increases. Reusing the system only once decreases the average cost by about 18%, however, the next reusability decreases the system mass by only 7%. Figures 10b-10c-10d show the values of the optimized design variables: thrust, expansion ratio and mixture ratio as a function of the reusability number. As the number of reusability increases, the optimization tends to favor more efficient vehicles even at the cost of higher dry weight. An increase in efficiency is primarily driven by two factors: lower gravitational losses and a gain in Isp. The three graphs are then explained as follows

- An increase of thrust diminishes the gravity losses at the cost of higher engine mass
- A higher expansion ratio increases the Isp at the cost of a higher engine mass
- A mixture ratio closer to the absolute optimal increases the Isp at the cost of an increase in tank mass

Figure 11 shows architectures #4 #5 #7 and #9 for two vehicles and how the ranking of the architectures changes as the number of reuses increases. At zero reuse, the ranking is 4-5-7-9. However for three reuses, the ranking is 7-9-4-5. The swapping around of the ordering of mission architectures is partially due to the fact that some architectures have expendable vehicles and some do not. In this particular case, architecture 4 and 5 both involve an expendable vehicle

Table 9 Selected architecture mission

	One-stage Fully expendable	Most efficient architecture 6 reuses		NASA proposed architecture 3 reuses		
Average mass per mission (t)	80.2	46.0		58.6		
Vehicle number	1	1	2	1	2	3
Total Mass (t)	80.2	50.8	16.1	36.0	26.1	13.3
Mix Ratio	7.29	6.82	6.86	6.67	6.59	6.73
Engine Thrust (kN)	216	189	44.0	139	246	52.5
Expansion Ratio	128	115	904	112	68.3	523
Dry Mass w/o payload (t)	13.0	10.3	1.71	8.64	3.43	1.41
Dry Mass w/ payload (t)	25.0	22.3	2.11	20.64	3.83	1.81
H2 Mass (t)	6.66	3.64	1.77	2.00	2.94	1.48
O2 Mass (t)	48.6	24.9	12.2	13.4	19.4	9.99
Fuel Tank + Coolant Mass (t)	2.95	1.62	0.786	0.890	1.30	0.658
Oxygen Tank + Coolant Mass (t)	0.432	0.221	0.108	0.119	0.172	0.0889
Engine Mass (t)	0.855	0.651	0.504	0.406	0.614	0.393
Engine Isp (s)	463	465	491	466	458	486
Structure Mass (t)	8.74	7.80	0.317	7.22	1.34	0.272

whereas architecture 7 and 9 have both vehicles reusable. Therefore for a low number of reuses, architectures 4-5 are preferred whereas for higher reusability architectures 7-9 tends to wins in terms of efficiency. It is worth keeping in mind that the objective function only considered the average mass of the vehicles and did not include any penalty originating from the maintenance of the system or the refurbishment of the vehicles. For example, the mass/performances of the engines were modeled independently of the number of reuse. In reality, reusable space vehicles tend to be more complex and so would incur higher development costs than expendable ones. In addition, as systems are made to be reusable more and more times, the system requirements get stronger and harder to comply with, increasing the development and operating cost. Proper implementation of these considerations with a penalty term in the objective function would most likely result in an optimal design that occurs at a finite number of reuses. Moreover, no penalty was considered for the complexity of the mission architectures. Tables 13 and 14 in the appendix show the main characteristics of the mission architectures for 2 and 3 vehicles. In future models, the objective function could have penalty terms related to the number of burns and the number of docking/undocking. Safety considerations should also be taken into account. For example, surface rendezvous and docking may be extremely challenging and carry high risks, this should factor into the optimization. This work also did not include any cost associated with keeping material (like fuel) in a lunar orbit.

VII. Conclusion

In order to design a reusable vehicle connecting the LOP-G with the lunar surface, an innovative methodology has been developed and presented in this paper. The methodology comprehends a dual approach. Firstly, the

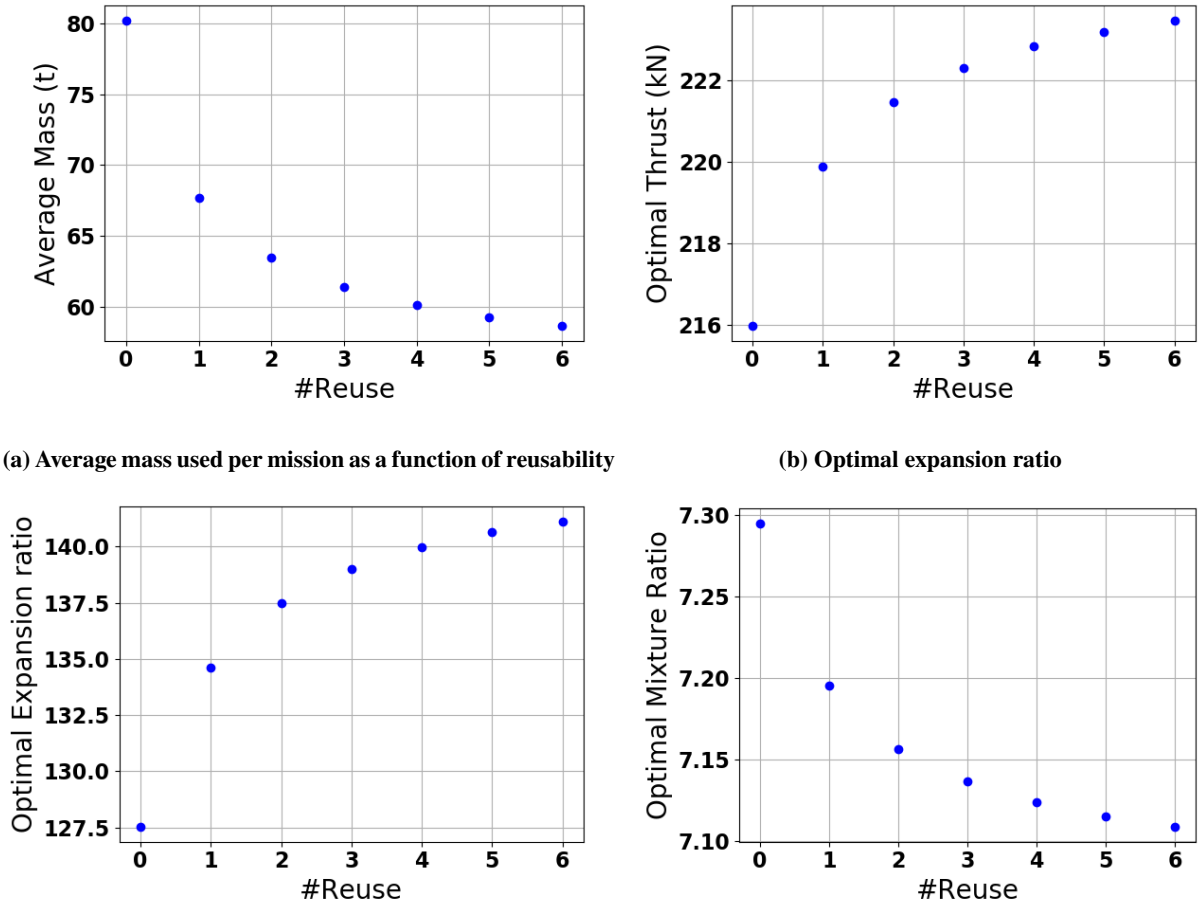

(a) Average mass used per mission as a function of reusability

(b) Optimal expansion ratio

(c) Optimal thrust

(d) Optimal mixture ratio

Fig. 10 Optimized objective function and design variables for a one stage vehicle

mission architectures are analyzed in a systematic way with simplified models. Then, a multidisciplinary analysis and optimization tool is developed to obtain the best design for the lander with respect to average mass used per mission. The two methods are then merged to obtain the best preliminary design for a family of architectures. The MDO process involved the 3 disciplines of propulsion, trajectory and structural/thermal analysis. The optimization variables were thrust, mixture ratio and expansion ratio of the vehicles. The objective function was chosen to be the average mass expended per mission with a number of reuses of the vehicles varying from 0 to 6. The effects of the reusability number on the optimization variables were observed and their behavior interpreted. With the 20 most promising architectures for 2 and 3 vehicles, a large database of results was established, ranking the different architecture by their average mass usage as a function of the reusability number. Interestingly, the ordering of the best architectures depends on the number of reuses. As part of the trajectory analysis software, an analytical expression of the gravity losses was obtained. With these results, a system engineer designing a lunar lander can use this paper and his own mission requirements to choose the most appropriate mission scenario for his/her situation. Future work will improve engineering models and consider

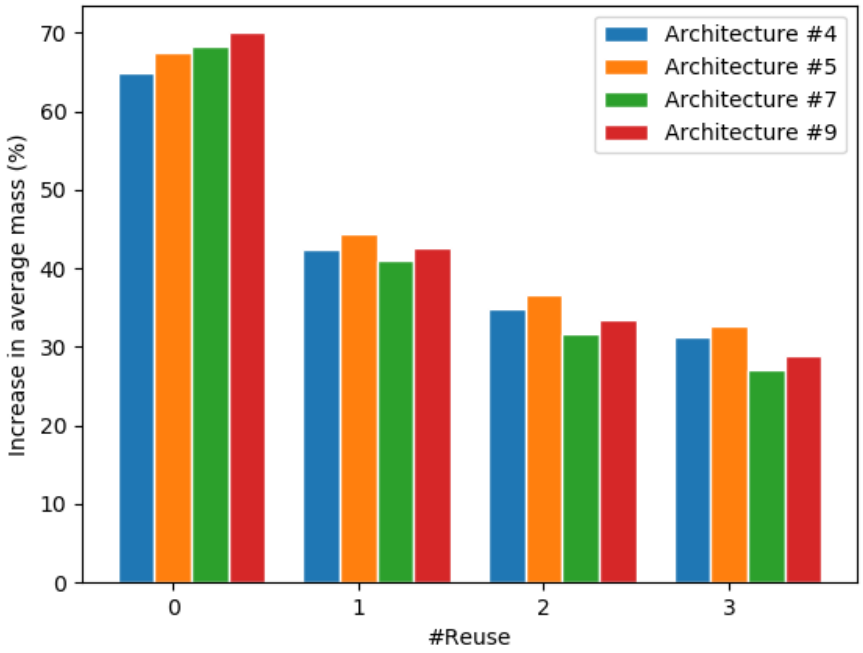

Fig. 11 Increase average mass for two vehicles architecture 4, 5, 7, 9. See Table 11

more propellant choices. Moreover, the objective function will integrate factors related to the characteristics of the mission architectures. Terms related to the cost of refurbishment of the vehicles should also be taken into account. A more thorough design of the most promising architectures will be done in future work.

Funding Sources

This work was possible due to the funding of Airbus DS, ArianeGroup and the SACLab at ISAE-SUPAERO

Acknowledgments

The help of the whole SACLab team at ISAE-SUPAERO is greatly appreciated. Special thanks goes to Alberto Fossa and Giuliana Miceli for their contribution of the optimal ascent/descent trajectory.

References

[1] T. Cichan, S. A. Bailey, A. Burch, N. W. Kirby, "Concept for a Crewed Lunar Lander Operating from the Lunar Orbiting Platform-Gateway," *69th International Astronautical Congress (IAC)*, 2018. doi:IAC-18.A5.1.4x46653.

[2] NASA, "America's Spacecraft for a New Generation of Explorers The Altair Lunar Lander," *NASAFacts*, 2007. URL `https://www.nasa.gov/pdf/289914main_fs_altair_lunar_lander.pdf`.

[3] Gray, J. S., Kenway, G. K., Mader, C. A., and Martins, J., *Aero-propulsive Design Optimization of a Turboelectric Boundary Layer Ingestion Propulsion System*, 2018 Aviation Technology, Integration, and Operations Conference. doi:10.2514/6.2018-3976, URL https://arc.aiaa.org/doi/abs/10.2514/6.2018-3976.

[4] Castellini, F., Riccardi, A., Lavagna, M., and Büskens, C., "Global and Local Multidisciplinary Design Optimization of Expendable Launch Vehicles," 2011. doi:10.2514/6.2011-1901.

[5] Brevault, L., Balesdent, M., and Hebbal, A., "Multi-Objective Multidisciplinary Design Optimization Approach for Partially Reusable Launch Vehicle Design," *Journal of Spacecraft and Rockets*, Vol. 0, No. 0, 0, pp. 1–17. doi:10.2514/1.A34601, URL https://doi.org/10.2514/1.A34601.

[6] Gray, J., Hearn, T., Moore, K., Hwang, J., Martins, J., and Ning, A., "Automatic Evaluation of Multidisciplinary Derivatives Using a Graph-Based Problem Formulation in OpenMDAO," 2014. doi:10.2514/6.2014-2042.

[7] Gray, J., Hwang, J., Martins, J., Moore, K., and Naylor, B., "OpenMDAO: An open-source framework for multidisciplinary design, analysis, and optimization," *Structural and Multidisciplinary Optimization*, 2019. doi:10.1007/s00158-019-02211-z.

[8] NTRS, "Lunar Lander Conceptual Design," *NASA-CR-172061, NAS 1.26:172061, EEI-87-171*, 1988. URL https://ntrs.nasa.gov/search.jsp?R=19880020470.

[9] NTRS, "Spacecraft mass estimation, relationships and engine data: Task 1.1 of the lunar base systems study," *NASA-CR-172051, NAS 1.26:172051, EEI-88-181*, 1988. URL https://ntrs.nasa.gov/search.jsp?R=19880020452.

[10] Robertson, B., Ramos, E. M., Díaz, M. J., and Mavris, D. N., "A Conceptual Design Study for an Unmanned , Reusable Cargo Lunar Lander," *70th International Astronautical Congress (IAC)*, 2019.

[11] Taylor, C., and de Weck, O., "Concurrent Trajectory and Vehicle Optimization: A Case Study of Earth-Moon Supply Chain Logistics," *46th AIAA/ASME/ASCE/AHS/ASC Structures, Structural Dynamics & Materials Conference*, 2005. doi:10.2514/6.2005-2202.

[12] Venkataraman, P., "Applied Optimization with Matlab Programming," *A Wiley - Interscience publication, John Wiley & Sons, New York*, 2001.

[13] NASA, "HUMAN LANDING SYSTEM BAA, INDUSTRY FORUM," *NASA-CR-172051, NAS 1.26:172051, EEI-88-181*, 2019. URL https://www.nasa.gov/sites/default/files/atoms/files/nasa_hls_baa_industry_forum_14feb2019.pdf.

[14] Martins, J. R. R. A., "A Short Course on Multidisciplinary Design Optimization," *Aerospace Dept. , University of Michigan*, 2012.

[15] Wächter, A., and Biegler, L. T., "Line Search Filter Methods for Nonlinear Programming: Motivation and Global Convergence," *SIAM Journal on Optimization*, Vol. 21, 2005, pp. 1–31.

[16] Gill, P. E., Murray, W., and Saunders, M. A., *SNOPT: An SQP Algorithm for Large-Scale Constrained Optimization*, Society for Industrial and Applied Mathematics, USA, 2005, Vol. 47, p. 99–131. doi:10.1137/S0036144504446096, URL https://doi.org/10.1137/S0036144504446096.

[17] Kraft, D., *A software package for sequential quadratic programming.*, Tech. Rep. DFVLR-FB 88-28, DLR German Aerospace Center – Institute for Flight Mechanics, Koln, Germany., 1988.

[18] Bryson, A. E., and Ho, Y.-C., *Applied Optimal Control: Optimization, Estimation, and Control*, 1975.

[19] Falck, R. D., and Gray, J. S., *Optimal Control within the Context of Multidisciplinary Design, Analysis, and Optimization*, 2018 Aviation Technology, Integration, and Operations Conference. doi:10.2514/6.2019-0976, URL https://arc.aiaa.org/doi/abs/10.2514/6.2019-0976.

[20] Herman, A. L., and Conway, B. A., *Direct Optimization Using Collocation Based on High-Order Gauss-Lobatto Quadrature Rules.*, Journal of Guidance, Control, and Dynamics 19.3, 1996.

[21] Garg, D. e. a., *A Unified Framework for the Numerical Solution of Optimal Control Problems Using Pseudospectral Methods*, Automatica 46.11, 2010.

[22] Ross, S., Koon, W., Lo, M., and Marsden, J., *Dynamical Systems, the Three-Body Problem, and Space Mission Design*, 2011.

[23] Wilhite, A., Tolson, R., Mazur, M., and Wagner, J., "Lunar Module Descent Mission Design," *Guidance, Navigation, and Control and Co-located Conferences. American Institute of Aeronautics and Astronautics*, 2008.

[24] Gomez, G., Jorba, A., Masdemont, J., and Simó, C., *Dynamics and mission design near libration points, advanced methods for collinear points*, 2001.

[25] Morrison, D. R., Jacobson, S. H., Sauppe, J. J., and Sewell, E. C., "Branch-and-bound algorithms: A survey of recent advances in searching, branching, and pruning," *Discrete Optimization*, Vol. 19, 2016, pp. 79 – 102. doi:https://doi.org/10.1016/j.disopt.2016.01.005, URL http://www.sciencedirect.com/science/article/pii/S1572528616000062.

[26] Orloff, R., "Apollo by the Numbers," *National Aeronautics and Space Administration. p. 22.*, 1996.

[27] Fortescue, P. W., and Stark, J. P. W., "Spacecraft Systems Engineering," *Chichester: Wiley*, 1995.

[28] Balesdent, M., "Multidisciplinary Design Optimization of Launch Vehicles," Theses, Ecole Centrale de Nantes (ECN), Nov. 2011. URL https://tel.archives-ouvertes.fr/tel-00659362.

[29] Mills, G., and Riesco, M., "Propellant Selection for the Lunar Lander Ascent Stage," *AIAA SPACE 2008 Conference & amp Exposition*, 2008. URL https://arc.aiaa.org/doi/abs/10.2514/6.2008-7906.

[30] S. Gordon, B. M., "Computer program for calculation of complex chemical equilibrium compositions and applications. Part 1: Analysis," *NASA technical report server*, 1994.

[31] Sutton, G. P., and Biblarz, O., *Rocket Propulsion Elements*, Wiley, 8 edition, 2010.

[32] R.W. Humble, W. J. L., G. N. Henry, "Space propulsion analysis and design," *McGraw-Hill Companies, inc*, 1195.

[33] NASA, "Orion Quick Facts," 2014. URL https://www.nasa.gov/sites/default/files/fs-2014-08-004-jsc-orion_quickfacts-web.pdf.

[34] Rapp, D., *Human Missions to Mars: Enabling Technologies for Exploring the Red Planet*, Springer, 2008.

[35] Radebaugh, R., "Cryocoolers: The state of the art and recent developments," *Journal of physics. Condensed matter: an Institute of Physics journal*, Vol. 21, 2009, pp. 164–219. doi:10.1088/0953-8984/21/16/164219.

[36] JPL, "Solar Cell and Array Technology for Future Space Science Missions," *NASA*, 2002. URL https://solarsystem.nasa.gov/resources/296/solar-cell-and-array-technologies-for-future-space-missions/.

[37] Davis, E. E., "Future orbital transfer vehicle technology study. Volume 2: Technical report," *NASA NTRS*, 1982. URL https://ntrs.nasa.gov/search.jsp?R=19820016399.

[38] Whitley, R. J., and Martínez, R. F., "Options for staging orbits in cislunar space," *2016 IEEE Aerospace Conference*, 2016, pp. 1–9.

[39] Izzo, D., "Revisiting Lambert's Problem," *Celestial Mechanics and Dynamical Astronomy*, 2014. doi:10.1007/s10569-014-9587-y.

[40] Robbins, H., "An analytical study of the impulsive approximation," *AIAA Journal 4 (8) 1417–1423*, 1966. URL https://arc.aiaa.org/doi/pdf/10.2514/3.3687.

[41] Bouhlel, M. A., Hwang, J. T., Bartoli, N., Lafage, R., Morlier, J., and Martins, J. R. R. A., "A Python surrogate modeling framework with derivatives," *Advances in Engineering Software*, 2019, p. 102662. doi:https://doi.org/10.1016/j.advengsoft.2019.03.005.

[42] Koelle, D. E., "The transcost-model for launch vehicle cost estimation and its application to future systems analysis," *Acta Astronautica*, Vol. 11, No. 12, 1984, pp. 803 – 817. doi:https://doi.org/10.1016/0094-5765(84)90100-0, URL http://www.sciencedirect.com/science/article/pii/0094576584901000.

[43] Digabel, S. L., and Wild, S. M., "A Taxonomy of Constraints in Simulation-Based Optimization," *arXiv: Optimization and Control*, 2015.

Appendix

Table 10 Results for one stage architecture.

# Reuse	0	1	2	3	4	5	6
% increase in average mass	74.5%	47.3%	38.1%	33.6%	30.8%	29.0%	27.7%

Table 11 Results for 2 stages architecture.

Reuse	0		1		2		3		4		5		6	
Ordering of the best architectures #1-#20, increase in relative mass %	#1	44.9%	#1	18.8%	#1	10.1%	#1	5.7%	#1	3.0%	#1	1.3%	#1	0.0%
	#2	50.1%	#2	23.7%	#2	14.9%	#2	10.4%	#2	7.8%	#2	6.0%	#2	4.7%
	#3	50.7%	#3	24.3%	#3	15.4%	#3	11.0%	#3	8.3%	#3	6.5%	#3	5.3%
	#4	64.8%	#7	40.9%	#7	31.7%	#7	27.1%	#7	24.3%	#7	22.5%	#7	21.2%
	#5	67.5%	#8	42.0%	#8	33.4%	#9	28.8%	#9	26.0%	#9	24.2%	#9	22.9%
	#8	67.5%	#4	42.4%	#9	33.4%	#8	29.1%	#8	26.5%	#8	24.8%	#8	23.6%
	#7	68.3%	#9	42.6%	#4	35.0%	#4	31.2%	#4	29.0%	#4	27.5%	#4	26.4%
	#6	69.5%	#5	44.3%	#5	36.6%	#5	32.7%	#5	30.4%	#5	28.8%	#5	27.7%
	#10	69.9%	#6	45.6%	#6	37.7%	#6	33.7%	#6	31.3%	#6	29.7%	#6	28.6%
	#9	70.0%	#11	49.1%	#11	42.2%	#20	38.0%	#20	35.1%	#20	33.2%	#20	31.9%
	#11	70.1%	#10	49.4%	#10	42.5%	#11	38.7%	#11	36.6%	#11	35.2%	#11	34.2%
	#13	72.6%	#13	50.7%	#20	42.7%	#10	39.1%	#10	37.1%	#10	35.7%	#10	34.7%
	#12	73.7%	#12	51.2%	#13	43.4%	#13	39.7%	#13	37.5%	#13	36.0%	#15	34.9%
	#14	75.1%	#14	51.8%	#12	43.7%	#12	39.9%	#15	37.7%	#15	36.1%	#13	35.0%
	#15	76.0%	#15	52.1%	#14	44.0%	#15	40.1%	#12	37.7%	#14	36.2%	#14	35.1%
	#20	80.3%	#20	52.1%	#15	44.1%	#14	40.1%	#14	37.7%	#12	36.2%	#12	35.1%
	#16	83.1%	#18	58.2%	#18	48.6%	#18	43.7%	#18	40.8%	#18	38.9%	#18	37.5%
	#17	84.8%	#16	58.9%	#16	50.8%	#19	46.6%	#19	43.6%	#19	41.7%	#19	40.3%
	#18	87.0%	#17	59.5%	#17	51.0%	#16	46.7%	#17	44.2%	#17	42.5%	#17	41.3%
	#19	90.1%	#19	61.1%	#19	51.4%	#17	46.7%	#16	44.3%	#16	42.6%	#16	41.5%

Table 12 Results for 3 stages architecture.

Reuse	0		1		2		3		4		5		6	
Ordering of the best architectures #1-#20, increase in relative mass %	#1	44.1%	#1	20.6%	#11	11.2%	#11	6.7%	#11	4.3%	#11	2.2%	#11	0.9%
	#2	44.8%	#14	20.9%	#14	12.5%	#14	8.3%	#14	5.7%	#14	4.0%	#14	2.8%
	#14	46.0%	#11	21.1%	#1	12.7%	#1	8.7%	#1	6.3%	#1	4.7%	#1	3.6%
	#4	46.3%	#2	21.7%	#2	14.0%	#9	9.9%	#9	7.2%	#9	5.4%	#9	4.1%
	#5	46.6%	#3	23.2%	#9	14.5%	#2	10.1%	#2	7.8%	#2	6.2%	#2	5.1%
	#11	46.8%	#9	23.6%	#3	15.3%	#3	11.3%	#3	9.0%	#3	7.4%	#3	6.2%
	#3	46.9%	#4	23.7%	#4	16.2%	#4	12.4%	#10	9.8%	#10	8.0%	#10	6.7%
	#17	47.7%	#5	24.1%	#5	16.5%	#10	12.6%	#16	10.0%	#16	8.2%	#16	6.9%
	#6	48.1%	#6	24.8%	#6	17.1%	#5	12.8%	#4	10.1%	#4	8.6%	#4	7.5%
	#7	48.4%	#7	25.2%	#10	17.2%	#16	12.8%	#5	10.5%	#5	9.0%	#5	7.9%
	#8	48.6%	#8	25.4%	#16	17.4%	#6	13.2%	#6	10.8%	#6	9.3%	#6	8.2%
	#15	49.1%	#15	25.5%	#7	17.5%	#15	13.6%	#15	11.2%	#15	9.6%	#15	8.4%
	#12	49.3%	#12	25.6%	#15	17.5%	#7	13.6%	#12	11.2%	#12	9.7%	#12	8.5%
	#18	49.5%	#17	25.6%	#8	17.6%	#12	13.6%	#7	11.3%	#7	9.7%	#7	8.6%
	#13	49.9%	#13	26.1%	#12	17.6%	#8	13.7%	#8	11.4%	#8	9.8%	#8	8.7%
	#9	50.6%	#10	26.4%	#13	18.2%	#13	14.2%	#13	11.8%	#13	10.2%	#13	9.0%
	#16	53.7%	#16	26.5%	#17	18.3%	#17	14.6%	#17	12.3%	#17	11.0%	#17	9.8%
	#10	53.8%	#18	27.4%	#18	20.0%	#18	16.3%	#18	14.1%	#18	12.6%	#18	11.5%
	#20	63.1%	#19	39.7%	#19	31.6%	#19	27.6%	#19	25.1%	#19	23.5%	#19	22.3%
	#19	63.9%	#20	40.7%	#20	33.3%	#20	29.5%	#20	27.3%	#20	25.8%	#20	24.7%

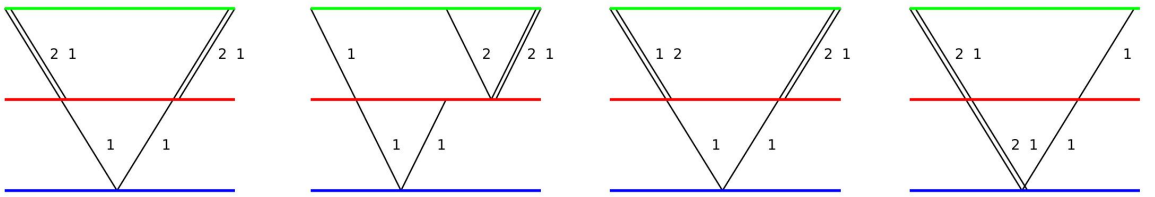

(a) Case 1 (b) Case 2 (c) Case 3 (d) Case 4

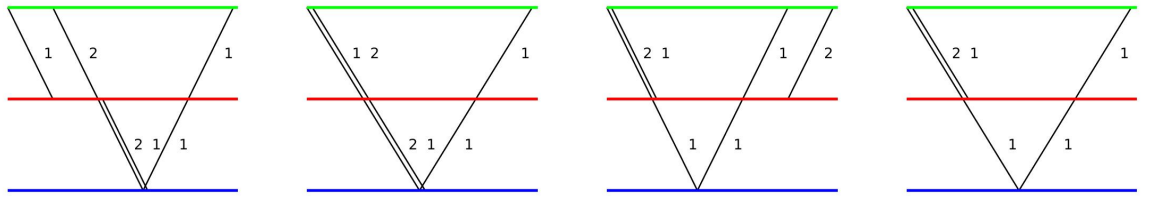

(e) Case 5 (f) Case 6 (g) Case 7 (h) Case 8

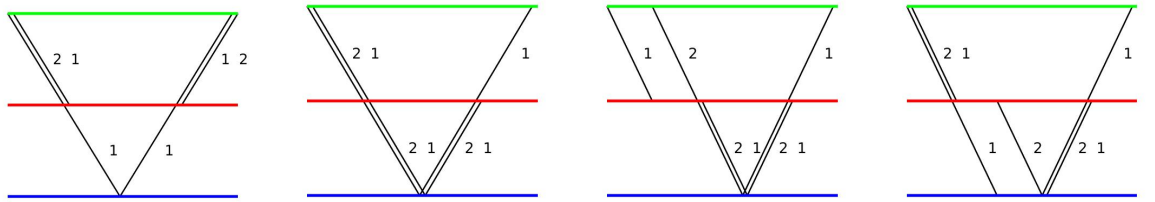

(i) Case 9 (j) Case 10 (k) Case 11 (l) Case 12

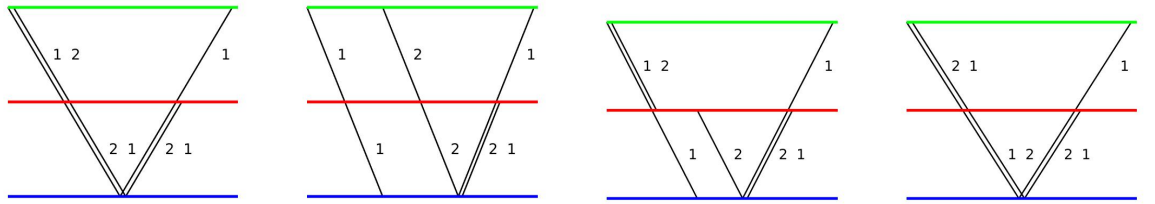

(m) Case 13 (n) Case 14 (o) Case 15 (p) Case 16

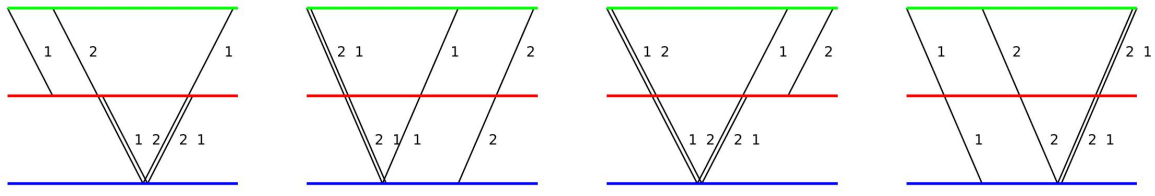

(q) Case 17 (r) Case 18 (s) Case 19 (t) Case 20

Fig. 12 Mission architectures for 2 vehicles

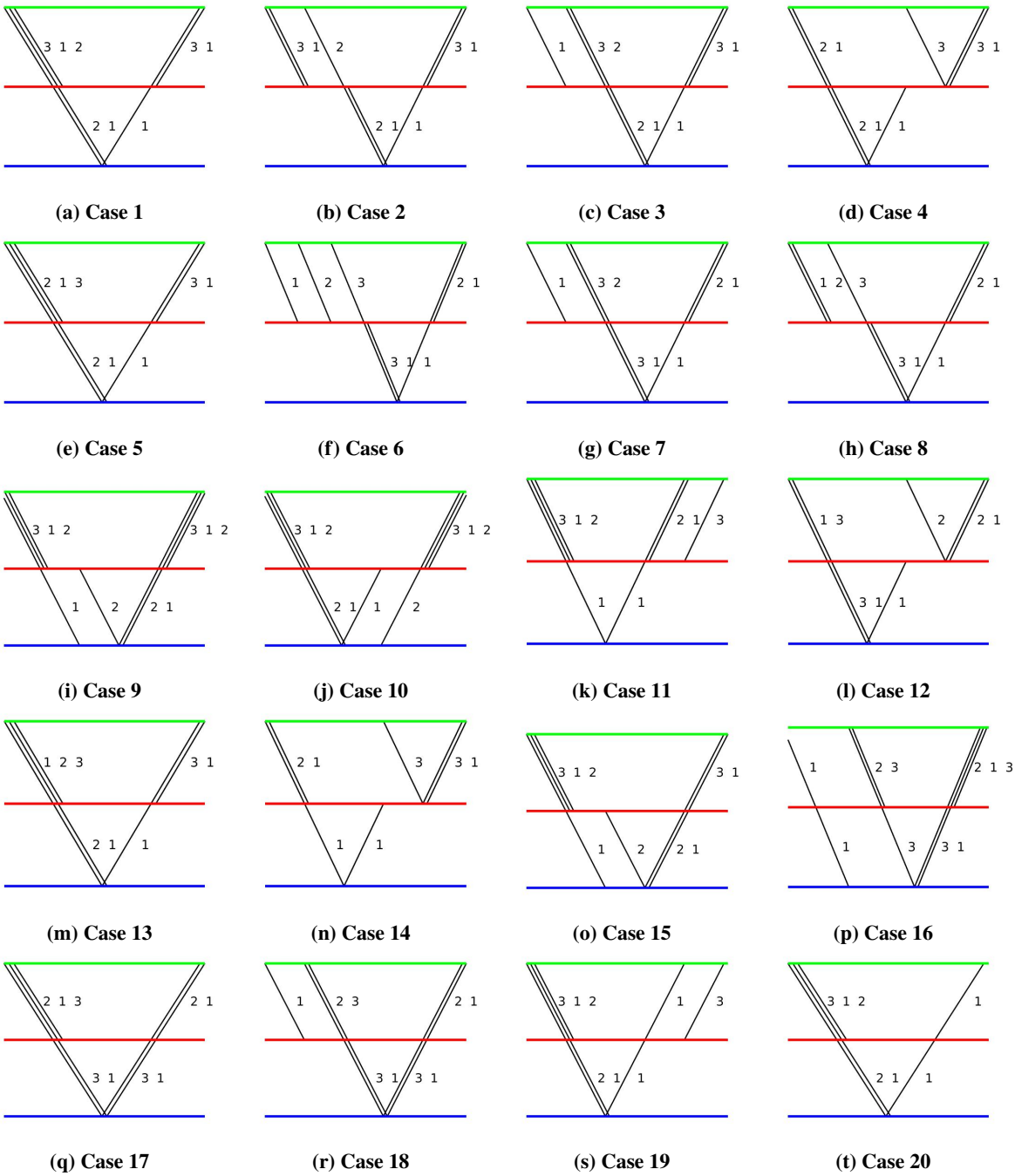

(a) Case 1 **(b) Case 2** **(c) Case 3** **(d) Case 4**

(e) Case 5 **(f) Case 6** **(g) Case 7** **(h) Case 8**

(i) Case 9 **(j) Case 10** **(k) Case 11** **(l) Case 12**

(m) Case 13 **(n) Case 14** **(o) Case 15** **(p) Case 16**

(q) Case 17 **(r) Case 18** **(s) Case 19** **(t) Case 20**

Fig. 13 Mission architectures for 3 vehicles

Table 13 Characteristics of mission architectures with 2 vehicles. The long burn column such as 2|3 means vehicle 1 needs 2 long burns and vehicle 2 needs 3 burns.

	Orbit Undocking	LOP-G Undocking	Surface Undocking	Orbit RDV + Docking	LOP-G RDV + Docking	Surface RDV + Docking	Long Burn	Expendable Vehicle
#1	1	1	0	1	1	0	2|2	0
#2	0	2	0	1	1	0	3|2	0
#3	1	1	0	1	1	0	3|1	0
#4	0	1	1	0	1	0	2|2	1
#5	0	2	1	1	1	0	3|2	1
#6	0	1	1	0	1	0	3|1	1
#7	1	1	0	0	2	0	3|2	0
#8	1	1	0	0	1	0	3|1	1
#9	1	1	0	1	1	0	3|1	0
#10	1	1	0	0	1	0	1|3	1
#11	1	2	0	1	1	0	2|3	1
#12	2	1	0	0	1	1	2|3	1
#13	1	1	0	0	1	0	2|2	1
#14	1	2	0	0	1	1	3|3	1
#15	2	1	0	0	1	1	3|3	1
#16	1	1	0	0	1	0	2|2	1
#17	1	2	0	1	1	0	3|2	1
#18	0	1	1	0	2	0	4|2	0
#19	1	1	0	0	2	0	3|2	0
#20	0	2	0	0	1	1	2|4	0

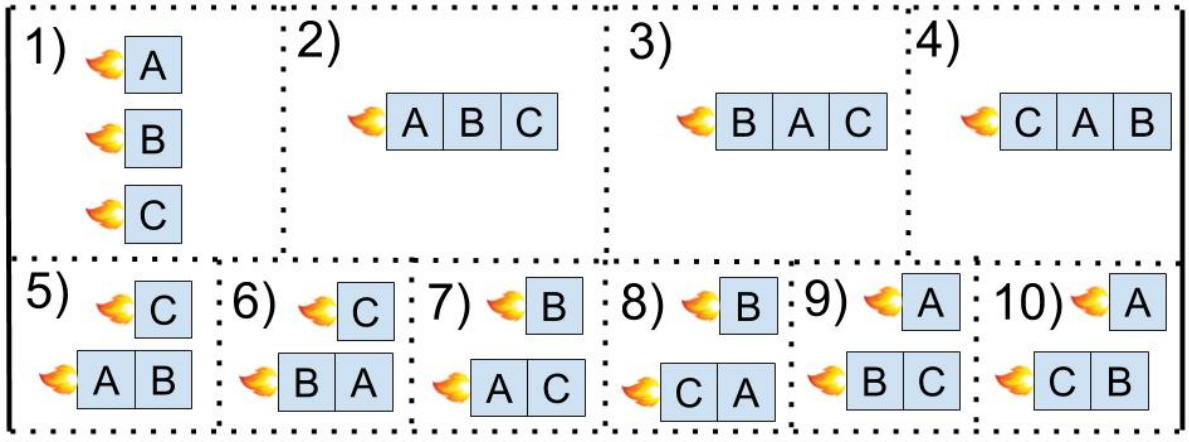

Fig. 14 Explicit construction of the 10 different possible transfer combinations with 3 vehicles, 1) to 10)

Table 14 Characteristics of mission architectures with 3 vehicles. The long burn column such as 3|2|1 means vehicle 1 needs 3 long burns, vehicle 2 needs 2 burns and vehicle 3 needs 1 burn.

	Orbit Undocking	LOP-G Undocking	Surface Undocking	Orbit RDV + Docking	LOP-G RDV + Docking	Surface RDV + Docking	Long Burn	Expendable Vehicle
#1	1	1	1	1	1	0	1|1|2	1
#2	1	2	1	2	1	0	1|2|2	1
#3	1	2	1	2	1	0	2|1|2	1
#4	0	2	1	1	1	0	1|2|2	1
#5	1	1	1	1	1	0	1|2|1	1
#6	0	3	1	2	1	0	2|2|2	1
#7	1	2	1	2	1	0	2|1|2	1
#8	1	2	1	2	1	0	2|1|2	1
#9	2	1	0	1	1	1	1|2|2	0
#10	1	1	1	2	1	0	1|2|2	0
#11	2	1	0	1	2	0	2|1|2	0
#12	0	2	1	1	1	0	2|2|1	1
#13	1	1	1	1	1	0	2|1|1	1
#14	1	2	0	1	1	0	2|1|2	1
#15	3	1	0	1	1	1	1|2|2	1
#16	1	2	0	1	1	1	2|2|2	1
#17	2	1	0	1	1	0	0|2|2	1
#18	2	2	0	2	1	0	1|2|2	1
#19	1	1	1	0	2	0	2|1|2	1
#20	1	1	1	0	1	0	2|1|1	2